

# Analysis on Temperature Field Simulation for Offset Cutting a Nanochannel at a Fixed Down Force on Single-crystal Silicon Using Three-dimensional Quasi-steady Molecular Statics Nanocutting Model

Zone-Ching Lin<sup>\*</sup>, Yu-Jheng Hu<sup>\*\*</sup> and Bo-Tang Zhao<sup>\*\*\*</sup>

**Keywords:** molecular statics, nanochannel, offset cutting, specific down force energy, temperature field

## ABSTRACT

The paper develops three-dimensional quasi-steady molecular statics nanocutting model to simulate offset cutting a nanochannel trapezium groove on single-crystal silicon at a fixed down force by a small probe. It is set that after a cutting pass is performed at a fixed down force on each cutting layer, the probe offsets rightwards to perform one more cutting pass, and then offsets leftwards to the middle position between the two passes aforesaid to perform cutting—this process is regarded as an offset cutting. The down force and cutting force of each cutting pass on the first cutting layer obtained from simulation of three-dimensional quasi-steady molecular statics nanocutting model are compared with the down force and cutting force of the cutting pass on the first cutting layer obtained from SDFE theoretical equation. The comparison has proved that it is feasible to use the three-dimensional quasi-steady molecular statics nanocutting model developed by the paper to simulate offset cutting of nanochannel trapezium groove at a fixed down force on single-crystal silicon by a small

probe. The paper considers that plastic heat and friction heat would be produced during cutting of every cutting pass. The plastic deformation heat of the paper can be calculated by multiplying the equivalent stress and equivalent strain of the workpiece of single-crystal silicon being cut. Focusing on the production method of friction heat on the surface of cutting tool for nanocutting of single-crystal silicon, the paper finds the calculation method of temperature rise produced from friction heat. After finding the sum of temperature rise produced from two heat sources, the paper achieves the total temperature rise of each atom of the single-crystal silicon workpiece being cut, and then analyzes the temperature field of each cutting pass on the first cutting layer when performing offset cutting at a fixed cutting force.

## INTRODUCTION

Shimada (1992) used two-dimensional atomic model and molecular dynamics to simulate dynamic simulation of microcutting and found its relation to chip formation. Considering atoms as nodes, Inamura et al. (1993) combined the Morse potential between atoms with the power of atoms to form total energy of atoms, and took this as a starting point to step by step induce finite element method (FEM) of atomic model. Lin and Huang (2004) once used molecular dynamics theory as the foundation, and further improved the FEM model of Inamura etc. (1993). Considering atoms as nodes and lattices as elements, they employed a self-developed equation of orthogonal nanocutting model to calculate the displacement of each molecule on the central cross-section of the cut workpiece, and then calculate strain.

If the time step of molecular dynamics was taken too small, the simulation process has to take a lot of time for calculation, and a problem of calculation will be produced. Therefore, gradually there were scholars using molecular statics method to simulate

*Paper Received September, 2019. Revised October, 2019. Accepted October, 2019. Author for Correspondence: Zone-Ching Lin.*

<sup>\*</sup> Professor, Department of Mechanical Engineering, National Taiwan University of Science and Technology, No.43, Keelung Rd., Sec.4, Da'an Dist., Taipei City 10607, Taiwan, email: zclin@mail.ntust.edu.tw

<sup>\*\*</sup> Graduated Student, Department of Mechanical Engineering, National Taiwan University of Science and Technology, No.43, Keelung Rd., Sec.4, Da'an Dist., Taipei City 10607, Taiwan, email: m1013248@mail.ntust.edu.tw

<sup>\*\*\*</sup> Graduated Student, Department of Mechanical Engineering, National Taiwan University of Science and Technology, No.43, Keelung Rd., Sec.4, Da'an Dist., Taipei City 10607, Taiwan, email: m10603217@mail.ntust.edu.tw

nanoscale studies, with an expectation to avoid the problems encountered by molecular dynamics. Kwon et al. (2004) studied the simulation of material property of static-load on atomic-grade balance, proposed combining atomic model with FEM model, and then used this model to simulate nanoscale problems. Jeng and Tan (2004) used molecular statics method and took the smallest energy principle in finite element as the framework to simulate the displacement and deformation process of nanoindentation. Lin and Hsu (2012) once combined molecular statics with the shape function in FEM to establish a simulation model of three-dimensional quasi-steady molecular statics orthogonal cutting to simulate the cutting force and cutting temperature of nanoscale orthogonal cutting of copper material.

Lin et al. (1995) developed an offset cutting method for fabricating nanoscale trapezium groove on single-crystal Si and a method of calculating cutting force based on SDFE theory. This study uses simulation model of three-dimensional quasi-steady molecular statics nanocutting to simulate the 1<sup>st</sup> to 3<sup>rd</sup> cutting passes of 1<sup>st</sup> cutting layer of offset cutting. The simulation results of cutting force and down force are compared with the results of cutting force and down force of the 1<sup>st</sup> to 3<sup>rd</sup> cutting passes obtained from SDFE theory.

The above studies have not mentioned any analysis of the stress and strain and temperature field on the cross-sections of workpiece after multiple-pass cutting by offset cutting method at a fixed down force. After obtaining the temperatures respectively risen from plastic heat and friction heat, they are added up to acquire the total heat increased, and then obtain the temperature distribution produced at different cutting passes on the 1<sup>st</sup> cutting layer after cutting of single-crystal silicon workpiece by offset cutting method at a fixed downforce.

### CALCULATION OF CUTTING FORCE AND DOWN FORCE BY USING SDFE THEORETICAL MODEL

SDFE is defined by multiplying the down force of the cutting tool of probe applied on workpiece by the cutting depth, and then dividing the workpiece. When nanocutting a V-shaped groove on single-crystal Si, Z axle is the down force direction for down press of AFM probe, whereas X axle is the cutting force direction for forward nanocutting of volume removed by down force of cutting tool [Lin and Hsu (2012)]. They found the SDFE value is a constant for different axle direction, and obtained the following equations:

$$SDFE = \frac{F_z \times \Delta dz_1}{\Delta V_1} = \frac{F_x \times \Delta dx_1}{\Delta V_1} \quad (1)$$

Down force in Z axle direction.

$$(F_z) = \frac{SDFE \times \Delta V_1}{dz_1} \quad (2)$$

$$(F_x) = \frac{F_z \times dz_1}{\Delta dx_1} = \frac{SDFE \times \Delta V_1}{\Delta dx_1} \quad (3)$$

Therefore, if the spherical radius of the tip of AFM probe is measured, and if  $\Delta dz_1$  is known as mentioned above, then  $\Delta dz_1$  and  $\Delta V_1$  can be calculated according to the spherical size of the tip of probe and by CAD software. The SDFE value acquired from experiment is substituted in SDFE equation (1) of different axle directions. Then, equations (2) and (3) are used to calculate the down force  $F_z$  and cutting force  $F_x$  for cutting of nanoscale trapezium groove on single-crystal Si for the 1<sup>st</sup>, 2<sup>nd</sup> and 3<sup>rd</sup> cutting passes of offset cutting method at the fixed down force using the SDFE theory. Figure 1 Shows the action force of different axle directions on V-shaped groove after the 1<sup>st</sup> cutting pass of nanocutting by AFM probe where  $\Delta dx_1 = r_c$  and  $r_c$  is crown circle radius of contact between workpiece and cutting tool,  $\Delta V_1$  is the volume removed by cutting,  $\Delta d_1$  is the cutting depth.

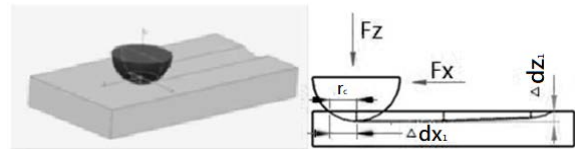


**Fig. 1.** Action force of different axle directions on V-shaped groove after the 1<sup>st</sup> cutting pass of nanocutting by AFM probe

Besides, the study uses AFM to cut V-shaped groove. The spherical radius of the tip of AFM probe is 150nm. Different down force values, 32.79 $\mu$ N, 38.5 $\mu$ N, 47.31 $\mu$ N are used to conduct cutting experiment of V-shaped groove on single-crystal Si substrate for the 1<sup>st</sup> cutting pass. AFM is used to measure the cutting depths at different down forces, and calculate the removed workpiece volume at each cutting depth. The SDFE theory and equation are further used to calculate the SDFE value of single-crystal Si, obtaining an average SDFE value of single-crystal Si around 0.01775( $\mu$ N  $\cdot$  nm/nm<sup>3</sup>). Therefore, the study supposes that the SDFE value of single-crystal Si is 0.01775( $\mu$ N  $\cdot$  nm/nm<sup>3</sup>).

### OFFSET CUTTING METHOD AT THE FIXED DOWN FORCE FOR FABRICATING NANOSCALE TRAPEZIUM GROOVE

The steps of offset cutting method at the fixed down force are that cutting is set to be carried out for one cutting pass at a constant down force on a cutting layer first, then it let the probe be offset rightwards to carry out cutting for one more cutting pass, and finally it let the probe leftwards to the middle position between the above two cutting passes to carry out the third cutting pass. Using the concept of step-by-step

approximation to numerical value of SDFE, the study calculates the cutting depth between cutting passes. In this way, between the cross-section shape of cutting by probe in the two cutting passes and the cross-section shape of cutting after offset to the middle position, upward bulginess and downward indentation are respectively caused at the bottom, as shown in Figure 2 for one cutting layer of offset cutting a nanoscale trapezium groove.  $H_1$  is the upward bulginess and  $H_2$  is the downward indentation at the bottom in Figure 2. It is proposed that the values of  $H_1$  and  $H_2$  are smaller than 0.54nm.

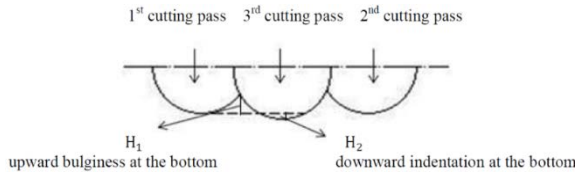


**Fig. 2.** Schematic diagram of upward bulginess and downward indentation at the bottom of nanoscale trapezium groove and three cutting passes for one cutting layer of offset cutting a nanoscale trapezium groove

### THREE DIMENSIONAL QUASI-STEADY MOLECULAR STATICS NANOCUTTING MODEL

#### Calculation of the Cutting Force of 3D Quasi-steady Molecular Statics Nanocutting Model

The three dimensional quasi-steady molecular statics nanocutting model of this paper adopts Morse potential energy of two-body potential energy as the basis for calculation of the action force between molecules.

The equation of Morse potential energy (Girifalco and Weizer, 1959) is expressed as follows:

$$\Phi(r_{ij}) = D\{e^{-2\alpha(r_{ij}-r_0)} - 2e^{-\alpha(r_{ij}-r_0)}\} \quad (4)$$

$D$ : binding energy

$\alpha$ : material parameter

$r_{ij}$ : distance between two atoms

$r_0$ : balance distance

This paper adopts Morse's two-body potential energy function to describe the interaction force between molecules when the diamond cutter is cutting a *silicon* workpiece. The Morse potential energy function parameters used between the carbon atoms of diamond cutter and the silicon atoms of the workpiece is shown in Table 1 (Zhang and Tanaka, 1997).

For the general potential energy function, when the distance between two atoms is greater than a certain distance, the action force between atoms will decrease rapidly. Therefore, we define the distance

cut-off radius  $r_c$ , and when the distance exceeds  $r_c$ , the action force is very small so it does not need to be calculated. In this way, the calculation can be tremendously simplified. According to the Morse potential used by this paper, the action force between two atoms can be expressed as equation (5):

$$F(r_{ij}) = -\frac{\partial\Phi(r_{ij})}{\partial r(r_{ij})} = 2D\alpha\{e^{-2\alpha(r_{ij}-r_0)} - e^{-\alpha(r_{ij}-r_0)}\} \quad (5)$$

When  $r_{ij} = r_0$ , the action force between atoms is just situated at a balance between attraction force. Both the cutting tool and workpiece material are at the situation of no action force. When  $r_{ij} < r_c$ , the diamond cutting tool and silicon material will produce action force. As the step of cutting tool moves forward, the so-called chip phenomenon is formed. By using equation (5), we can infer that the action force between two atoms can be expressed as equation (6):

$$\vec{F}_i = \sum_{i=1}^n \vec{F}_{ij} \delta(r_{ij}) \quad \text{if } \begin{matrix} r_{ij} > r_c, & \delta = 0 \\ r_{ij} < r_c, & \delta = 1 \end{matrix} \quad (6)$$

$i$ : a number given to the carbon atom of cutting tool.

$j$ : a number given to the silicon atom in material.

$n$ : quantity of silicon atoms.

$r_{ij}$ : distance between two atoms.

**Table 1.** Morse potential energy function parameters between diamond cutter and atoms of silicon workpiece material.

	Si-Si	Si-C
$D$ : binding energy (ev)	3.032	0.435
$\alpha$ : material parameter ( $\text{\AA}^{-1}$ )	0.7981	4.6487
$r_0$ : equilibrium distance between atoms ( $\text{\AA}$ )	4.208	1.9475

The numerical value of the produced action force is divided into 3 axial component forces,  $\vec{F}_x$ ,  $\vec{F}_y$  and  $\vec{F}_z$ , forming equation (7) as follows:

$$\vec{F}_i = \vec{F}_{x_i} + \vec{F}_{y_i} + \vec{F}_{z_i} \quad (7)$$

where  $\vec{F}_{x_i}$ ,  $\vec{F}_{y_i}$  and  $\vec{F}_{z_i}$  are the component forces of action force in X, Y and Z directions

Of course, after cutting is performed for a period of time, not only one atom of silicon workpiece is affected by the Morse force of the diamond cutting tool. Therefore, after the unknown force vector in the silicon workpiece affected by the Morse force of the diamond cutting tool is sequentially added to the force vectors of this group of atoms towards the silicon atoms within the cut-off radius itself, the sum of unknown force vectors can be acquired, and decomposed to be component  $F_x$  in X direction, component  $F_y$  in Y direction, and component  $F_z$  in Z

direction. Let them be zero respectively, and then there is a quasi-steady balance equation formed.

This paper proposes the use of optimization concept to find the most suitable displacement position. To find the most suitable displacement position by optimization search method, we firstly have to fix a searching range. Since the feeding of each step does not exceed 0.002Å in this paper and it is not easy for the atom to go through another atom to conduct deformation, this paper supposes that each feeding does not exceed the distance of 1/2 lattice constant, so as to search the most suitable force balance deformation and displacement position for the feeding of each step. Hooke-Jeeves' search method is employed to carry out the search.

Focusing on the nanoscale cutting simulation of single-crystal silicon, this paper proposes the following methods. First of all, the new coordinates of atoms after displacement in each step are calculated. Then, the atoms are numbered. According to finite element method (FEM), segmented grids are arrayed and numbered one by one. Based on these numbers, they are substituted in cut-off radius equation, Morse potential function, force balance as well as stress and strain equations in proper order. The calculated equivalent strain and Morse force are respectively substituted in the equations for calculation of plastic heat source and friction heat source. Adding these two heat sources up, the temperature field distribution of workpiece can be found.

### Calculation of Equivalent Stress and Equivalent Strain of the Quasi-steady Molecular Statics Nanocutting Model

After using molecular statics to calculate the newly displaced position of the atom in each step, strain-displacement relational equation can be used to obtain the atomic-level equivalent strain.

Therefore, after derivation, the strain displacement relational equation is as follows:

$$\{\varepsilon\} = [B]\{\delta\} \quad (8)$$

where  $\{\varepsilon\}$  is the strain matrix of element,  $[B]$  is the displacement-strain relationship matrix and  $\{\delta\}$  is the node displacement matrix.

It can be seen that after the displacement component of silicon atoms has been acquired from the quasi-steady nanocutting model, the strain of element can be obtained from equation (8).

Then, from the acquired strain of element made up of silicon atoms in the equation, the equivalent strain can be further calculated. Regarding the equation for the relationship curve between equivalent strain and equivalent stress, this paper uses equation (9) of the equivalent stress-equivalent strain curve acquired from Aly (2006) simulation experiment of the numerical tensile value of nanoscale silicon film, as the basis. According to equation (9) and the equivalent strain calculated above, the equivalent

stress produced under the equivalent strain of each element can be calculated.

$$\begin{cases} \bar{\sigma} = 687.5043\varepsilon^3 - 490.9562\varepsilon^2 + 147.4096\varepsilon + 7.7323 & \varepsilon \leq 0.25 \\ \bar{\sigma} = 46.2108\varepsilon + 13.8598 & \text{else} \end{cases} \quad (9)$$

### Calculation of Temperature Rise of the Cut Silicon Workpiece During Nanocutting

This paper carries out quasi-steady molecular statics simulation in three-dimensional way, and the initial temperature of workpiece and cutting tool are both supposed to be at room temperature (300K).

In the nanocutting process, this paper supposes that the main heat is produced from two heat sources as follows:

1. Plastic deformation heat produced from quasi-plastic deformation, which is caused by deformation between atoms of workpiece.
2. Friction heat produced between workpiece atoms and tool atoms.

This paper supposes that in the workpiece atoms in contact with the tool face, friction heat is produced in the various atoms with the adjacent distance between the workpiece atoms bearing Morse force and the tool atoms being smaller than 1 Å. Therefore,  $\Delta d_{fi}$  is supposed to be the displacement increment of workpiece atoms on the tool face in tangential direction. Thus,  $\Delta d_{fi} = V_{fi} \Delta t$ . As mentioned above, friction heat is supposed to be produced from the friction between the atoms on cutting tool and the workpiece atoms. The calculation method is shown as follows:

$$Q_{fi} = \frac{F_{fi} \Delta d_{fi}}{J} \quad (10)$$

where  $F_{fi}$ : friction force on the tool face after decomposing the Morse force borne by workpiece atoms.  
 $V_{fi}$ : tangential speed of the interface between workpiece atoms and the tool face atoms.  
 $\Delta t$ : time interval.

For the product of multiplying the equivalent stress by equivalent strain of each element obtained in the nanocutting simulation model, this paper regards it as quasi-plastic heat source. Therefore, within the time  $\Delta t$  of workpiece, this paper supposes that the temperature rise caused by quasi-plastic deformation is:

$$\Delta T_d = \frac{\int \bar{\sigma} \varepsilon \Delta t}{Jc\rho} \quad (11)$$

where  $c$  denotes the specific heat, and  $\rho$  denotes the density of material.

Since the abovementioned friction heat is produced on the various workpiece atoms contacting along the tool face direction, they are distributed to the nearest cutting tool and workpiece atoms in  $\alpha_w/\alpha_t$  proportion. Thus, the temperature rise distributed to the workpiece and the tool face are  $\Delta T_{wi}$  and  $\Delta T_{ti}$  respectively, being equation (12) as follows (Lin et al.,1995):

$$\Delta T_{wi} = \frac{\alpha_w}{\alpha_w + \alpha_t c_w \rho_w v_w} Q_{fi}$$

$$\Delta T_{ti} = \frac{\alpha_w}{\alpha_w + \alpha_t c_t \rho_t v_t} Q_{fi} \quad (12)$$

where  $\alpha_w = \left(\frac{k_w}{c_w \rho_w}\right)^{\frac{1}{2}}$ ,  $\alpha_t = \left(\frac{k_t}{c_t \rho_t}\right)^{\frac{1}{2}}$

In the equation,  $v_w$  and  $v_t$  are the volume of particles on the interface of workpiece and cutting tool respectively, whereas  $k_w$  and  $k_t$  are the thermal conductivity coefficients of workpiece and cutting tool respectively.

## RESULTS AND DISCUSSIONS

### Comparing the Down Force and Cutting Force Calculated by SDFE Theoretical Model with Those Simulation Results of Three-Dimensional Quasi-steady Molecular Statics Nanocutting

The paper firstly applies SDFE theory to simulate offset cutting of nanoscale trapezium groove. After simulation of the cutting depths of the 1<sup>st</sup>, 2<sup>nd</sup> and 3<sup>rd</sup> cutting passes on the 1<sup>st</sup> cutting layer, the study calculates the values of upward bulginess and downward indentation at the bottom as well as the cutting force and down force by SDFE theory. Therefore, using a probe with tip radius 2nm, and taking the case of the 1<sup>st</sup> cutting pass on the 1<sup>st</sup> cutting layer at 0.6432nm, then the fixed down force calculated by SDFE theory is 32.16Nn. The paper carries out simulation of offset cutting by SDFE theoretical model, with related calculation results shown in Table 2.

Besides, this study uses three-dimensional quasi-steady molecular statics nanocutting to simulate the down force and cutting force of the 1<sup>st</sup> cutting pass and 3<sup>rd</sup> cutting pass on the 1<sup>st</sup> cutting layer following the cutting depth with a probe tip radius 2nm. Using a probe with tip radius 2nm, the study simulates three-dimensional quasi-steady molecular statics nanocutting of 1<sup>st</sup> cutting pass of offset cutting method on the 1<sup>st</sup> cutting layer, with the cutting depth at 0.6432nm, and makes analysis of the simulation.

**Table 2.** Related calculation results of offset cutting by SDFE theory at the fixed down force on the 1<sup>st</sup> cutting layer with a probe tip radius 2nm.

Case for cutting depth of 1 <sup>st</sup> cutting pass on the 1 <sup>st</sup> cutting layer	Case 1
Cutting depth of the 1 <sup>st</sup> and 2 <sup>nd</sup> cutting passes on the 1 <sup>st</sup> cutting layer	0.6432
Cutting depth of the 3 <sup>rd</sup> cutting pass on the 1 <sup>st</sup> cutting layer	0.7481
Rightward offset amount of 2 <sup>nd</sup> cutting pass of offset cutting (nm)	3.0
Leftward offset amount of 3 <sup>rd</sup> cutting pass of offset cutting (nm)	1.5
Down force calculated by SDFE theory (nN)	32.16
Cutting force of 1 <sup>st</sup> cutting pass calculated by SDFE theory (nN)	14.12
Cutting force of 3 <sup>rd</sup> cutting pass calculated by SDFE theory (nN)	15.24
Upward bulginess at the bottom of nanoscale trapezium groove on the 1 <sup>st</sup> cutting layer (nm)	0.311
Downward indentation at the bottom of nanoscale trapezium groove on the 1 <sup>st</sup> cutting layer (nm)	0.105

Based on the simulation results of three-dimensional quasi-steady molecular statics nanocutting, the paper can obtain the cutting force  $F_x$  in X axle direction and the down force  $F_z$  in Z axle direction under steady cutting state. As above mentioned offset cutting method, the cutting depths of the 1<sup>st</sup> and 2<sup>nd</sup> cutting passes on the 1<sup>st</sup> cutting layer are the same. Hence, the paper only carries out simulation of three-dimensional quasi-steady molecular statics nanocutting for the 1<sup>st</sup> and 3<sup>rd</sup> cutting passes of offset cutting method on the 1<sup>st</sup> cutting layer. The obtained simulation result of cutting force ( $F_x$ ) and down force ( $F_z$ ) of each step at cutting depth 0.6432nm on the 1<sup>st</sup> cutting layer by using three-dimensional quasi-steady molecular statics nanocutting is shown in Figure 3.

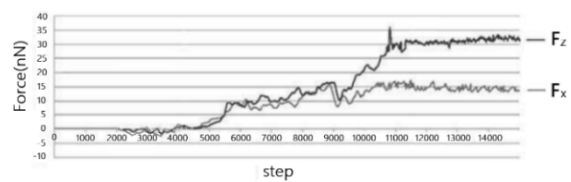


**Fig.3.** Simulation results of down force and cutting force of probe with tip radius 2nm at cutting depth 0.6432nm of 1<sup>st</sup> cutting pass on the 1<sup>st</sup> cutting layer

In order to prove the feasibility of its self-developed equation of SDFE theoretical model to estimate down force and cutting force, the average cutting force and down force acquired from the simulation results of three-dimensional quasi-steady molecular statics nanocutting are compared with the cutting force and down force calculated by the equations of cutting force and down force of SDFE theory. Table 3 shows that the stable average cutting force and stable average down force of the 1<sup>st</sup> cutting pass on the 1<sup>st</sup> cutting layer calculated in simulation of three-dimensional quasi-steady molecular statics nanocutting of single-crystal Si under the conditions with tip radius of probe at 2 nm, and cutting depth at 0.6432 nm is compared with the cutting force and down force calculated by equations of SDFE theory. In Table 3, it also shows that the difference between them are small.

**Table 3.** Comparison of average cutting force and average down force of nanoscale trapezium groove on single-crystal Si of the 1<sup>st</sup> cutting pass on the 1 cutting layer calculated by simulation model of molecular statics nanocutting, with the cutting force calculated by SDFE theoretical equation, and the difference between them

Case for cutting depth of 1 <sup>st</sup> cutting pass on the 1 <sup>st</sup> cutting layer	Case 1
Depth of the 1 <sup>st</sup> cutting pass on the 1 <sup>st</sup> cutting layer (nm)	0.6432
Down force of the 1 <sup>st</sup> cutting pass calculated by SDFE equation (nN)	32.16
Stable Average down force of the 1 <sup>st</sup> cutting pass on the 1 <sup>st</sup> cutting layer in simulated model of molecular static nanocutting (nN)	33.61
Difference (%)	4.5
Cutting force of the 1 <sup>st</sup> cutting pass calculated by SDFE equation (nN)	14.12
Stable average cutting force of the 1 <sup>st</sup> cutting pass on the 1 <sup>st</sup> cutting layer in simulated model of molecular static nanocutting (nN)	14.63
Difference (%)	3.61

**Table 4.** Comparison of average down force and average cutting force of the 3<sup>rd</sup> cutting pass on the 1<sup>st</sup> cutting layer of offset cutting of nanoscale trapezium groove on single-crystal Si calculated by the simulation model of three-dimensional quasi-steady molecular statics nanocutting, with the down force and cutting force calculated by SDFE theoretical equation, and the difference between them

Case for cutting depths of 3 <sup>rd</sup> cutting pass on the 1 <sup>st</sup> cutting layer	Case 1
Depth of the 3 <sup>rd</sup> cutting pass on the 1 <sup>st</sup> cutting layer (nm)	0.7481
Down force of the 3 <sup>rd</sup> cutting pass calculated by SDFE equation (nN)	32.16
Stable Average down force of the 3 <sup>rd</sup> cutting pass on the 1 <sup>st</sup> cutting layer in simulated model of molecular static nanocutting (nN)	33.27
Difference (%)	3.45
Cutting force of the 3 <sup>rd</sup> cutting pass calculated by SDFE equation (nN)	15.24
Stable average cutting force of the 3 <sup>rd</sup> cutting pass on the 1 <sup>st</sup> cutting layer in simulated model of molecular static nanocutting (nN)	15.84
Difference (%)	3.93

The study also supposes that the 1<sup>st</sup> and 2<sup>nd</sup> cutting passes of offset cutting of nanoscale trapezium groove on si substrate by AFM probe have similar simulation conditions. Since the simulated cutting processes of the 1<sup>st</sup> and 2<sup>nd</sup> cutting pass of offset cutting are both simulated cutting of a single groove, the cutting force and down force of the 1<sup>st</sup> cutting pass on the 1<sup>st</sup> cutting layer calculated by the simulation model of three-dimensional quasi-steady molecular statics nanocutting are regarded as the same as those of the 2<sup>nd</sup> cutting pass. Using a probe with tip radius 2nm, the study carries out simulation of three-dimensional quasi-steady molecular statics nanocutting for the 3<sup>rd</sup> cutting pass of offset cutting on the 1<sup>st</sup> cutting layer, with the cutting depth of the 3<sup>rd</sup> cutting pass at 0.7481 nm and makes analysis of the simulation. Based on the simulation results, the paper calculates the cutting force  $F_x$  in X axle direction and the down force  $F_z$  in Z axle direction under steady cutting state. Table 4 shows the comparison of the stable average down force  $F_z$  and stable average cutting force  $F_x$  of the 3<sup>rd</sup> cutting pass on the 1<sup>st</sup> cutting layer obtained from the simulation results of three-dimensional quasi-steady molecular statics nanocutting, with the down force and cutting force calculated by SDFE theoretical equation, and the difference between them. In Table 4, it shows the difference

between them are small. It is proved that the simulation results of average down force and average cutting force using the simulation model of three-dimensional quasi-steady molecular statics nanocutting are reasonable.

**Analysis on Equivalent Strain and Equivalent Stress at Different Cutting Passes on The 1<sup>st</sup> Cutting Layer of the Cut Single-Crystal Silicon Using Offset Cutting Method at A Fixed Down Force After Simulation of Three-Dimensional Quasi-Steady Molecular Statics Nanocutting Simulation Model**

The paper uses an AFM diamond probe with tip radius 2nm, and employs offset cutting method at a fixed down force to make a cutting depth 0.6432 nm at the 1<sup>st</sup> cutting pass on the 1<sup>st</sup> cutting layer. Simulation is carried out using three-dimensional quasi-steady molecular statics nanocutting simulation model. When simulated cutting is up to the 13,000<sup>th</sup> step, we can observe the distribution trend of equivalent strain and equivalent stress on the workpiece's X-axial cross-section (A-A section) in cutting direction and its Y-axial cross-section (B-B section) in vertical cutting direction. In the process of cutting a depth of 0.6432 nm at the 1<sup>st</sup> cutting pass, the maximum numerical values of equivalent strain produced on A-

A section and B-B section in the middle position of cutting tool are around 0.93 and 0.91, and that of equivalent stress are around 56.83 GPa and 55.9 GPa.

The paper uses an AFM diamond probe with tip radius 2nm and employs offset cutting method at a fixed down force to make a cutting depth 0.7481 nm at the 3<sup>rd</sup> cutting pass on the 1<sup>st</sup> cutting layer. When simulated cutting is up to the 13,000<sup>th</sup> step, we can observe the distribution trend of equivalent strain and equivalent stress on the workpiece's X-axial cross-section (A-A section) in cutting direction and its Y-axial cross-section (B-B section) in vertical cutting direction, as shown in Figure 4. As seen from A-A section in Figure 4, in the place where the chip on the left hand side is close to the surface of cutting tool when the single-crystal silicon workpiece contacts the cutting tool during advancement of cutting tool on X-axial direction, its equivalent stress value and equivalent strain value are greater. Besides, as seen from A-A section and B-B section in Figure 4, the shape of contour line distribution trend of equivalent strain and equivalent stress is quite close to the appearance of cutting tool. The deeper the penetration, the smaller its value. This is due to displacement of atoms produced for being pushed by cutting tool after the cutting tool cuts to the workpiece. Hence, strain and stress are produced on the cut surface. However, when the atoms go deeper down to the cut surface, since the cutting action of cutting tool is smaller, equivalent strain and equivalent stress are smaller. As to the stress and strain distribution state on B-B section, since the appearance of cutting tool is spherical, their distribution appears to be bilaterally symmetrical. The difference in value between the symmetrical positions on the left and right hand sides is very small. Therefore, only the left hand side of B-B section in Figure 4 is taken to indicate the positions of maximum equivalent strain and maximum equivalent stress. In the process of cutting a depth of 0.7481 nm at the 3<sup>rd</sup> cutting pass, the maximum numerical value of equivalent strain produced on A-A section and B-B section in the middle position of cutting tool is around 0.94 and 0.92, and that of equivalent stress are around 57.51 GPa and 56.56 GPa.

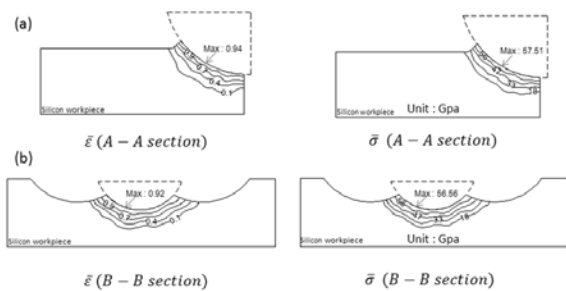
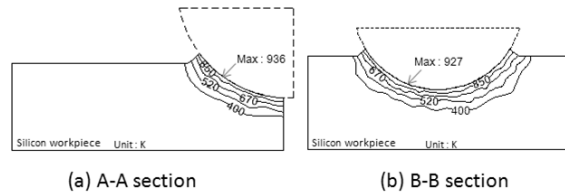


**Fig. 4.** (a) Equivalent stress  $\bar{\sigma}$  and equivalent strain  $\bar{\epsilon}$  on A-A section; and (b) equivalent stress  $\bar{\sigma}$  and equivalent strain  $\bar{\epsilon}$  on B-B section, in the middle position at the 13,000<sup>th</sup> step at a cutting depth 0.7481nm at the 3<sup>rd</sup> cutting pass

### Calculation and Analysis of Cutting Temperature of Different Cutting Passes on the 1<sup>st</sup> Cutting Layer Using Offset Cutting Method at A Fixed Down Force

Based on the application of quasi-steady molecular statics nanocutting simulation model developed by the paper as mentioned above and the calculation method of temperature rises of the heat sources of each atom of the cut workpiece. The paper simulates calculation of single-crystal silicon workpiece material. After using offset cutting method at a fixed down force to cut a trapezium groove at different cutting passes on the 1<sup>st</sup> cutting layer, the temperature rise produced from plastic heat and the temperature rise produced from friction heat on the cross-section in the middle are both taken. When the cutting force turns stable, the paper adds up the total temperature rise produced from plastic heat and the total temperature rise produced from friction heat of single-crystal silicon workpiece material, and achieves the total temperature risen by various atoms of the cut workpiece. After room temperature 300K is added, contour lines can be drawn to indicate the temperature field distribution curve diagram of the cross-section in the middle of the cut single-crystal silicon workpiece, and analysis can be made accordingly.

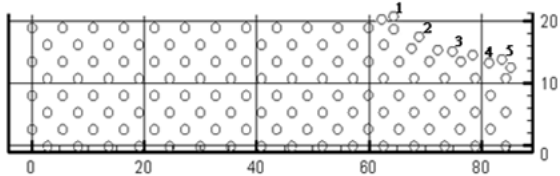
As mentioned above, the paper takes the 13,000<sup>th</sup> step of cutting to calculate the equivalent stress and equivalent strain of A-A section and B-B section of single-crystal silicon workpiece, and further calculates the temperature rise and total temperature rise produced from plastic heat and friction heat on both A-A section and B-B section, and then analyzes the temperature field distribution. Figure 5 shows the temperature rise produced from plastic heat and friction heat on both A-A section and B-B section of single-crystal silicon workpiece when the cutting depth at the 1<sup>st</sup> cutting pass is 0.6432 nm. After room temperature 300K is added, a diagram of final total temperature field is obtained. The highest temperatures produced on A-A section and B-B section are 936K and 927K respectively.



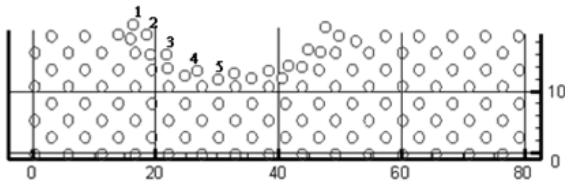
**Fig. 5.** Final total temperature field produced after adding room temperature 300K to the temperatures risen from plastic heat and friction heat on (a) A-A section and (b) B-B section, in the middle of the 13,000<sup>th</sup> step when the cutting depth at the 1<sup>st</sup> cutting pass is 0.6432 nm

Figure 6 and Figure 7 respectively show the diagrams of A-A section and B-B section when using AFM diamond probe tool with tip radius 2nm to make

a cutting depth 0.6432 nm on the single-crystal silicon workpiece by offset cutting method at a fixed down force at the 1<sup>st</sup> cutting pass on the 1<sup>st</sup> cutting layer after simulation is up to the 13,000<sup>th</sup> step. In the figures, the atoms with numbers are the single-crystal silicon workpiece atoms having contacted with the surface of cutting tool as analyzed by the paper.



**Fig. 6.** Diagram of A-A section of single-crystal silicon workpiece cut with a cutting depth 0.6432 nm at the 1<sup>st</sup> cutting pass when simulation in the cutting direction is up to the 13,000<sup>th</sup> step



**Fig. 7.** Diagram of B-B section of single-crystal silicon workpiece cut with a cutting depth 0.6432 nm at the 1<sup>st</sup> cutting pass when simulation in the cutting direction is up to the 13,000<sup>th</sup> step

Table 5 and Table 6 respectively show the final total temperatures (K) obtained after adding room temperature 300K to the temperatures ( $\Sigma\Delta T$ ) risen by plastic heat and friction heat of atoms of the cut single-crystal silicon workpiece. As known from Table 5, the temperature risen by plastic heat of No. 3 atom on A-A section in the cutting direction of cutting tool is 598K and the temperature risen by friction heat is 38K, so the total temperature rise of 636K is maximum. As known from Table 6, the temperature risen by plastic heat of No. 4 atom on B-B section in the cutting direction of vertical cutting tool is 591K and the temperature risen by friction heat is 36K, so the total temperature rise of 627K is maximum.

**Table 5.** Different risen temperatures and final total temperatures on A-A section with a cutting depth 0.6432 nm at the 1<sup>st</sup> cutting pass when cutting in a cutting direction is up to the 13,000<sup>th</sup> step

Atom No.	Temperature risen from plastic heat $\Sigma\Delta T_d$ (K)	Temperature risen from friction heat $\Sigma\Delta T_w$ (K)	Total temperature rise $\Sigma\Delta T$ (K)	Final total temperature (K)
1	535	41	576	876
2	581	32	613	913
3	598	38	636	936
4	549	36	585	885
5	522	39	561	861

**Table 6.** Different risen temperatures and final total temperatures on B-B section with a cutting depth 0.6432 nm at the 1<sup>st</sup> cutting pass when cutting in a cutting direction is up to the 13,000<sup>th</sup> step

Atom No.	Temperature risen from plastic heat $\Sigma\Delta T_d$ (K)	Temperature risen from friction heat $\Sigma\Delta T_w$ (K)	Total temperature rise $\Sigma\Delta T$ (K)	Final total temperature (K)
1	564	34	598	898
2	551	38	589	889
3	548	37	585	885
4	591	36	627	927
5	563	32	595	895

Applying the above method, the paper calculates the temperature rise produced from plastic heat and friction heat on A-A section in the middle of workpiece and B-B section in vertical cutting direction at the 3<sup>rd</sup> cutting pass on the 1<sup>st</sup> cutting layer when using offset cutting method at a fixed down force to cut single-crystal silicon workpiece material in cutting direction up to the 13,000<sup>th</sup> step. The positions of A-A section and B-B section are shown in Figure 8. When the cutting force reaches a stable step after cutting is up to the 13,000 step, the paper simulates calculation of the total temperature rise produced from plastic heat and friction heat of single-crystal silicon workpiece material obtained at the 3<sup>rd</sup> cutting pass. After the total temperature rise is added with room temperature 300K, contour lines can be drawn to indicate the temperature field distribution curve diagram of the single-crystal silicon workpiece after addition of room temperature 300K to the temperature rise produced from plastic heat and friction heat on A-A section and B-B section of the cut single-crystal silicon workpiece. In the final analysis of atoms on B-B section, since the appearance of cutting tool is spherical, their distribution appears to be bilaterally symmetrical. The difference in value between the symmetrical positions on the left and right hand sides is very small. Therefore, only the left hand side of B-B section in Figure 8 is taken as the maximum temperature. Similarly, in Figure 9 and Figure 10, only the atoms on the left hand side are taken to analyze the temperature rise produced from plastic heat and friction heat.

The paper takes the 13,000<sup>th</sup> step of cutting to observe the temperature field distribution trend on A-A section and B-B section of single-crystal silicon workpiece. Figure 8 shows the temperature field diagram acquired after room temperature 300K is added to the temperature rise produced from plastic heat and friction heat on A-A section and B-B section of single-crystal silicon workpiece with a cutting depth 0.7481 nm at the 3<sup>rd</sup> cutting pass. The highest temperatures produced on A-A section and B-B section are 949K and 937K respectively.

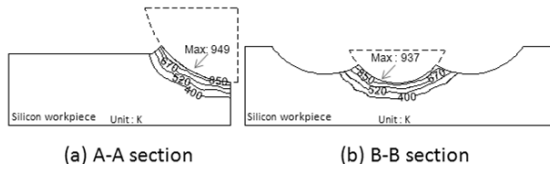


**Fig. 8.** Final total temperature field after adding room temperature 300K to the temperatures risen from plastic heat and friction heat on (a) A-A section and (b) B-B section in the middle of the 13,000<sup>th</sup> step with a cutting depth 0.7481 nm at the 3<sup>rd</sup> cutting pass

Figure 9 and Figure 10 respectively show the diagrams of A-A section and B-B section when using AFM diamond probe tool with tip radius 2nm to make a cutting depth 0.7481 nm on the single-crystal silicon workpiece by offset cutting method at a fixed down force at the 3<sup>rd</sup> cutting pass on the 1<sup>st</sup> cutting layer after simulation is up to the 13,000<sup>th</sup> step. In the figures, the atoms with numbers are the single-crystal silicon workpiece atoms having contacted with the surface of cutting tool as analyzed in the paper.

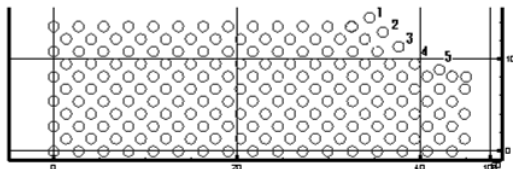


**Fig. 9.** Diagram of A-A section of single-crystal silicon workpiece cut with a cutting depth 0.7481 nm at the 3<sup>rd</sup> cutting pass when simulation in the cutting direction is up to the 13,000<sup>th</sup> step

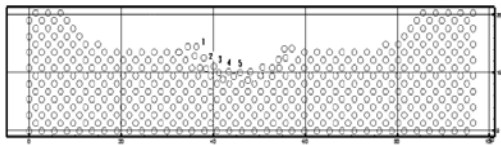


**Fig. 10.** Diagram of B-B section of single-crystal silicon workpiece cut with a cutting depth 0.7481 nm at the 3<sup>rd</sup> cutting pass when simulation in vertical cutting direction is up to the 13,000<sup>th</sup> step

Table 7 and Table 8 respectively show the final total temperatures (K) obtained after adding room temperature 300K to the temperatures ( $\Sigma\Delta T$ ) risen from plastic heat and friction heat of atoms of the cut single-crystal silicon workpiece at the 3<sup>rd</sup> cutting pass. As known from Table 7, the temperature risen from plastic heat of No. 3 atom on A-A section in the cutting direction of cutting tool is 608K. After it is added with friction heat 41K, the total temperature rise 694K is maximum. As known from Table 8, the temperature risen from plastic heat of No. 4 atom on B-B section in the cutting direction of vertical cutting tool is 597K. After it is added with friction heat 40K, the total temperature rise 637K is maximum.

**Table 7.** Different risen temperatures and final total temperatures on A-A section with a cutting depth 0.7481 nm at the 3<sup>rd</sup> cutting pass when cutting in a

cutting direction up to the 13,000<sup>th</sup> step

Atom No.	Temperature risen from plastic heat $\Sigma\Delta T_d$ (K)	Temperature risen from friction heat $\Sigma\Delta T_w$ (K)	Total temperature rise $\Sigma\Delta T$ (K)	Final total temperature (K)
1	544	37	581	881
2	590	42	632	931
3	608	41	649	949
4	558	40	598	898
5	530	36	566	866

**Table 8.** Different risen temperatures and final total temperatures on B-B section with a cutting depth 0.7481 nm at the 3<sup>rd</sup> cutting pass when cutting in a cutting direction up to the 13,000<sup>th</sup> step

Atom No.	Temperature risen from plastic heat $\Sigma\Delta T_d$ (K)	Temperature risen from friction heat $\Sigma\Delta T_w$ (K)	Total temperature rise $\Sigma\Delta T$ (K)	Final total temperature (K)
1	573	36	609	909
2	560	39	599	899
3	556	41	597	897
4	597	40	637	939
5	572	35	607	907

## CONCLUSION

After analysis of the simulation results aforesaid, important results are obtained as follows:

1. The paper uses a theoretical model of specific down force energy (SDFE) in different axial directions to calculate the down force value and cutting force value at the 1<sup>st</sup> cutting pass and the 3<sup>rd</sup> cutting pass on the 1<sup>st</sup> cutting layer; and then uses three-dimensional quasi-steady molecular statics nanocutting simulation model to simulate calculation of the down force value and cutting force value at different cutting passes on the 1<sup>st</sup> cutting layer cut by offset cutting method at a fixed down force, to make comparison between them. It is found that the difference of them are small. Therefore, it is proved feasible for the paper to use offset cutting method at a fixed down force of three-dimensional quasi-steady molecular statics nanocutting simulation model to carry out cutting of single-crystal silicon nanochannel.
2. It is found that during cutting, the temperature risen from plastic heat of the cut single-crystal silicon workpiece is greater than the temperature risen from friction heat. Therefore, the temperature rise of different atoms of the cut single-crystal silicon workpiece mainly comes from the temperature risen from the heat produced from plastic deformation. From the distribution of contour lines of total temperature rise at the 1<sup>st</sup> cutting pass and the 3<sup>rd</sup> cutting pass, it can be seen that the shape of contour lines of temperature distribution is close to the shape of the cutting tool's surface. And the

shape of contour line distribution of equivalent stress and equivalent strain is also close to the shape of the cutting tool's surface. Besides, the atom positions of the maximum total temperature rise on A-A section at the 1<sup>st</sup> cutting pass and that at the 3<sup>rd</sup> cutting pass are both calculated, whereas the atom positions of the maximum total temperature rises on B-B section at the above two passes are also calculated.

## ACKNOWLEDGEMENT

The authors would like to thank the support from Ministry of Science and Technology, Taiwan. (MOST 105-2221-E-011-045-MY3)

## REFERENCES

- Aly, M. F., Ng, E., Veldhuis, S.C. and Elbestawi, M.A. "Prediction of Cutting Forces in the Micromachining of Silicon Using a Hybrid Molecular Dynamic-finite Element Analysis Force Model", *International Journal of Machine Tools and Manufacture*, Vol.46, Issue 14, pp.1727-1739 (2006).
- Girifalco, L.A. and Weizer, V.G. "Application of the Morse Potential Function to Cubic Metals," *Phys. Rev.*, Vol. 114, pp. 687-690 (1959).
- Inamura, T., Takezawa, N. and Kumaki, N. "Mechanics and energy dissipation in nanoscalecutting", *CIRP Annals - Manufacturing Technology*, Vol.42, pp.79-82 (1993).
- Jeng, Y.R. and Tan, C.M. "Study of Nanoindentation Using FEM Atomic Model", *Journal of Tribology*, pp.767-774 (2004).
- Kwon, Y.W. and Jung, S.H. "Atomic model and coupling with continuum model for static equilibrium problems", *Computers & Structures*, Vol.82, pp.1993-2000 (2004).
- Lin, Z.C. and Huang, J.C. "Anano-orthogonal Cutting Model Based on a Modified Molecular Dynamics Technique", *Nanotechnology*, Vol.15, pp.510-519 (2004).
- Lin, Z.C. and Hsu, Y.C. "Analysis on Simulation of Quasi-steady Molecular Statics Nanocutting Model and Calculation of Temperature Rise During Orthogonal Cutting of Single-crystal Silicon", *CMC: Computers, Materials, & Continua*, Vol.27, pp.143-178 (2012).
- Lin, Z.C., Pan, W.C. and Lo, S.P. "A Study of Orthogonal Cutting with Tool Flank Wear and Sticking Behavior on the Chip-Tool Interface", *Journal of Materials Processing Technology*, Vol.52, No.2-4, pp.524-538 (1995).
- Shimada, S., "Molecular dynamics analysis as compared with experimental results of micromachining", *CIRP Annals-Manufacturing Technology*, Vol.41, pp.117-120 (1992).
- Zhang, L. and Tanaka, H. "Towards a deeper understanding of wear and friction on the atomic scale- a molecular dynamics analysis", *Wear*, Vol.221, pp. 44-53 (1997).

# 分子靜力學三維準穩態奈米切削模式模擬固定下壓力偏移加工單晶矽奈米流道凹槽之溫度模擬分析

林榮慶 胡育政 趙柏棠  
國立台灣科技大學 機械工程系

## 摘要

本文發展出分子靜力學三維準穩態奈米切削模式，模擬 AFM 探針切削單晶矽奈米流道梯形凹槽的固定下壓力偏移加工。本文以固定下壓力之偏移循環加工方法，加工單晶矽基板奈米流道梯形凹槽，其為設定每切削層在固定下壓力下切削一道次，然後將探針向右偏移再切削一道次，再將探針向左往回偏移至前述兩道次中間位置切削加工，做為一個偏移加工。本文再用分子靜力學三維準穩態奈米切削模式模擬比下壓能理論採用的切削深度，模擬所得之第一切削層各切削道次之下壓力及切削力和用比下壓能理論之公式所得之第一切削層切削道次之下壓力及切削力相比較，驗證本文發展的分子靜力學三維準穩態奈米切削模式模擬 AFM 探針切削單晶矽奈米流道梯形凹槽的固定下壓力偏移加工為合理可行。本文考慮各切削道次加工時，會產生塑性熱及摩擦熱。本文塑性變形熱可由被切削工件單晶矽，其等效應力與等效應變之乘積計算出。本文針對奈米切削單晶矽刀面上產生摩擦熱的方法，並計算因摩擦熱源產生的溫度提升之方法。本文再將兩種熱源所產生之溫度提升加總計算後，得到被切削單晶矽工件各原子提升之總溫度，再進行固定下壓力偏移加工的第一切削層各切削道次的溫度場分析。